†Electronic Supporting Information for

Vibrational analysis and chemical activity of paracetamol-oxalic acid cocrystal based on monomer and dimer calculations: DFT and AIM approach

Karnica Srivastava[1], Manishkumar R. Shimpi[2], Anubha Srivastava[1], Poonam Tandon[*1], Kirti Sinha[1] and Sitaram P. Velaga[2]

[1]Physics Department, University of Lucknow, Lucknow 226 007, India
[2]Department of Health Sciences Luleå University of Technology, S-971 87, Luleå, Sweden

Experimental details of DSC and XRPD of prepared cocrystal are given below and DSC plot of paracetamol and paracetamol-oxalic acid cocrystal are shown in Fig.S1 and Fig. S2 shows the XRPD plot of cocrystal. Optimized structure of paracetamol (monomer) and oxalic acid (monomer) are shown in Fig.S3, S4 .Experimental and calculated IR and Raman spectra of paracetamol (monomer) and oxalic acid (monomer) are shown in Fig.S5, S6, S7, S8. Fig.S9 shows the experimental structure of oxalic acid. The experimental structure of paracetamol forming hydrogen bonding with neighboring molecule is shown in Fig.S10. The molecular graph of monomer of paracetamol oxalic acid cocrystal (PRA-OXA) using AIM program is given in Fig.S11 Molecular electrostatic potential (MEPS) surface of paracetamol (monomer) and monomer of cocrystal are given in Fig.S12, S13. HOMO and LUMO of paracetamol (monomer) and PRA-OXA cocrystal (monomer) and its energy band gap are given in Fig.S14,S15.The experimental and calculated geometric parameters of monomer and dimer+2OXA of cocrystal is given in Table S1. Theoretical and experimental vibrational wave number of paracetamol (monomer) and oxalic acid (monomer) are listed in Table S2, S3. The experimental and theoretical wave number of the cocrystal using monomer and dimer+2OXA model is given in Table S4. Selected Lewis orbitals (occupied bond orbital or lone pair) with percentage ED over bonded atoms (ED_X, ED_Y in %), hybrid NBOs with s and p character in % for monomer of co-crystal are listed in Table S5. Geometrical parameters for hydrogen bonds in dimer+2OXA of co-crystal are given in Table S6. Reactivity descriptors as Fukui functions (fk^+, fk^-), local softnesses (sk^+, sk^-), local electrophilicity indices (ωk^+, ωk^-) for paracetamol (monomer) and PRA-OXA (monomer), using Hirshfeld atomic charges are given in Table S7,S8.

Differential scanning calorimetry (DSC)

The DSC profiles of the solid samples were generated in the range of (30–200 °C) using a TA Q1000 DSC instrument with a refrigerated cooling unit. Temperature calibration was performed using an indium metal standard at the respective heating rate. Samples (1–2 mg) were crimped in non-hermetic aluminum pans and scanned at a heating rate of 10 °C/min under a continuously purged dry nitrogen atmosphere (flow rate 50 mL/min) using a similar empty pan as a reference. The data were collected in triplicate for each sample and analysed using a TA Instruments Universal Analysis 2000 version 4.5A software.

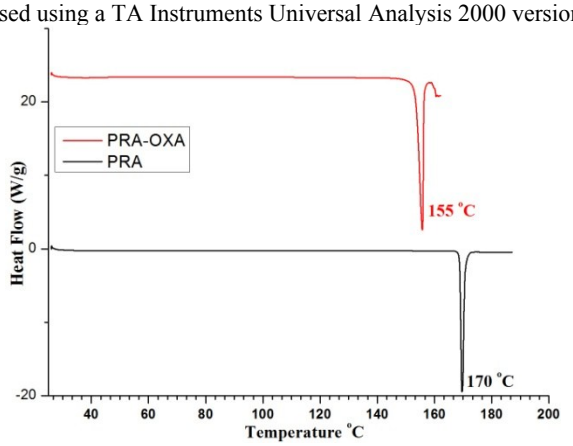

Fig. S1 DSC plot of PRA (melting point 170 ^{O}C) and PRA-OXA cocrystal (melting point 155^{O}C)

Powder X-ray Diffraction (PXRD).

PXRD patterns for the samples were collected using an Empyrean X-ray diffractometer (PANalytical, The Netherlands) equipped with a PIXel3D detector and a monochromatic Cu Kα radiation X-Ray tube (1.54056). The tube voltage and amperage were set at 45 kV and 40 mA, respectively. Samples were prepared for analysis by pressing a thin layer of the sample onto a metal sample

holder. Instrument calibration was performed using a silicon reference standard. Each sample was scanned 2θ range of 5o to 40o, increasing at a step size of 0.02o 2θ. The data were process using HighScore Plus Version 3.0 software (PANalytical, The Netherlands).

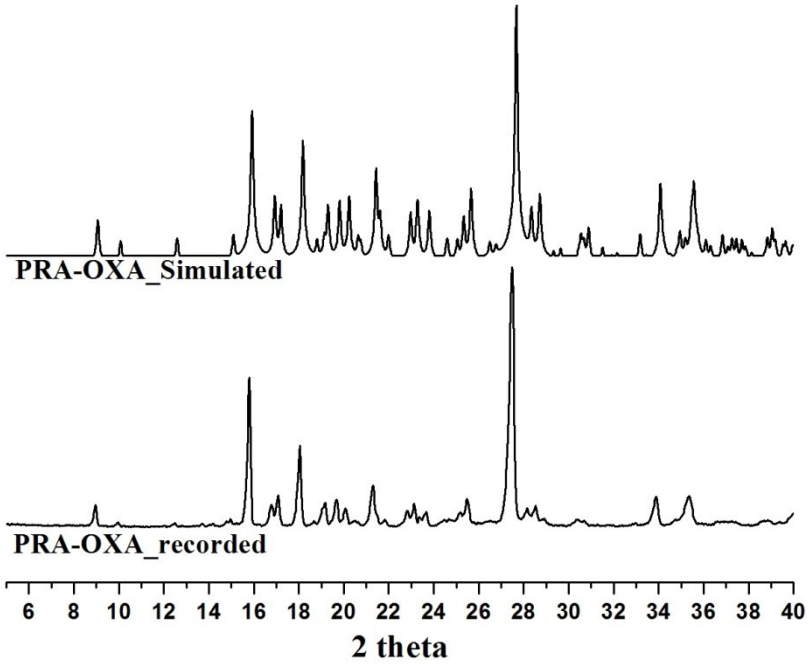

Fig. S2 XRPD overlapped of prepared PRA-OXA cocrystal with its simulated pattern.

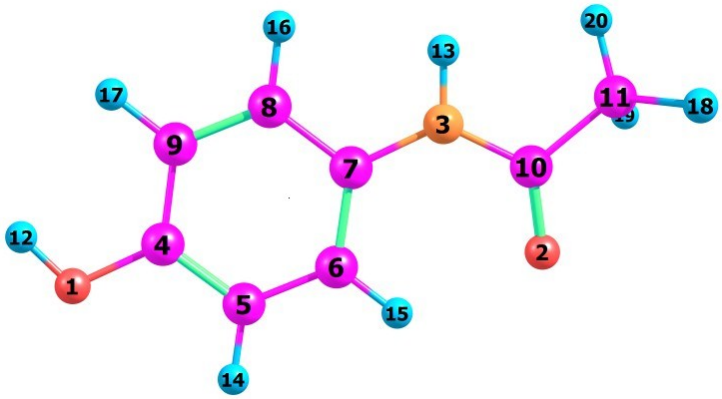

Fig. S3 Optimized structure of paracetamol

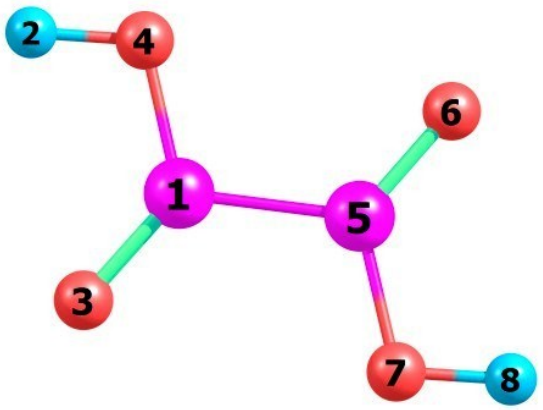

Fig. S4 Optimized structure of oxalic acid

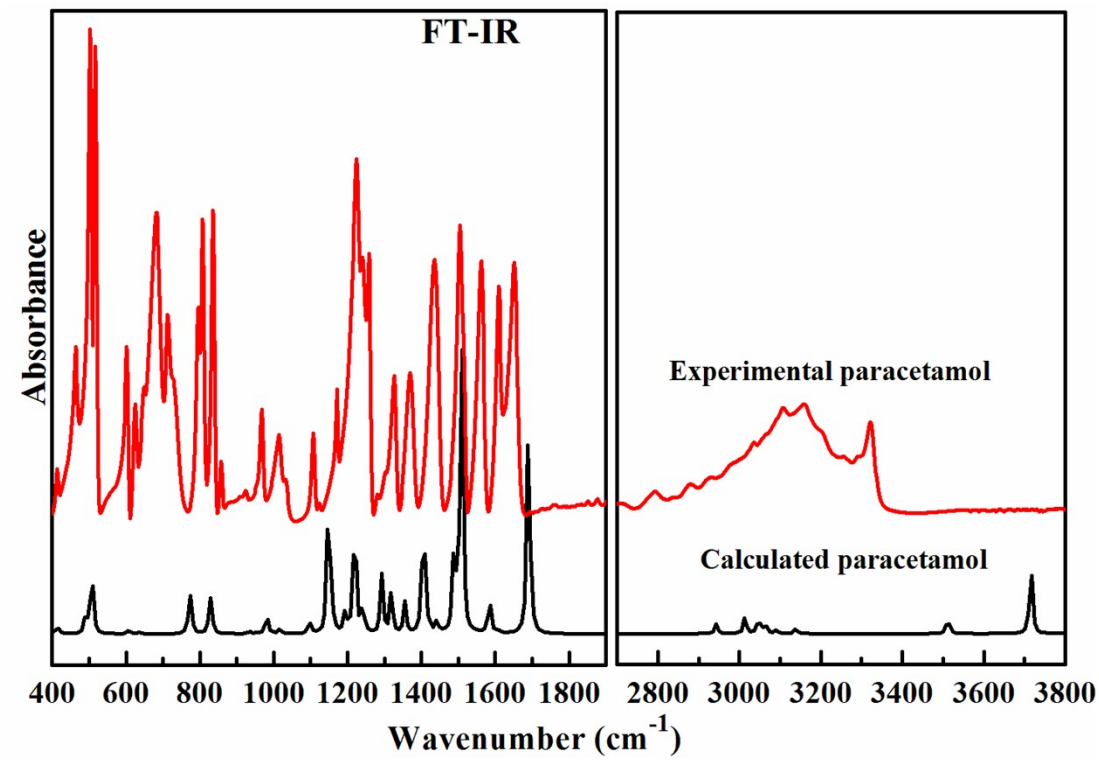

Fig. S5 Experimental and calculated (scaled) IR absorbance spectra of paracetamol in the region 400-1900cm^{-1} and 2700-3800cm^{-1}.

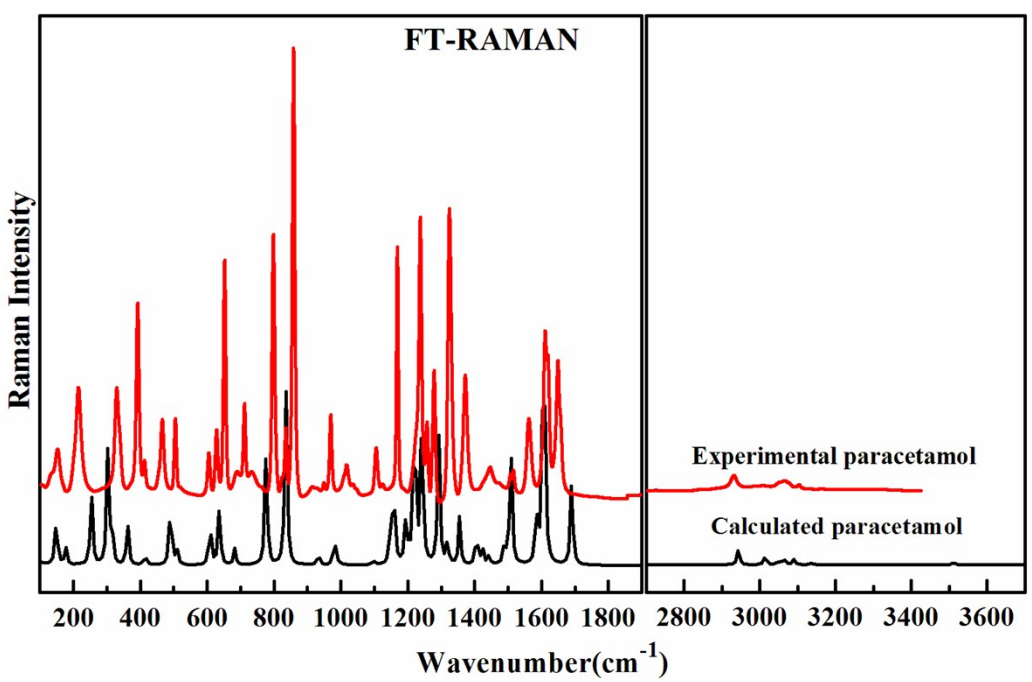

Fig. S6 Experimental and calculated (scaled) Raman scattering spectra of paracetamol in the region 100-1900cm^{-1} and 2700-3700cm^{-1}.

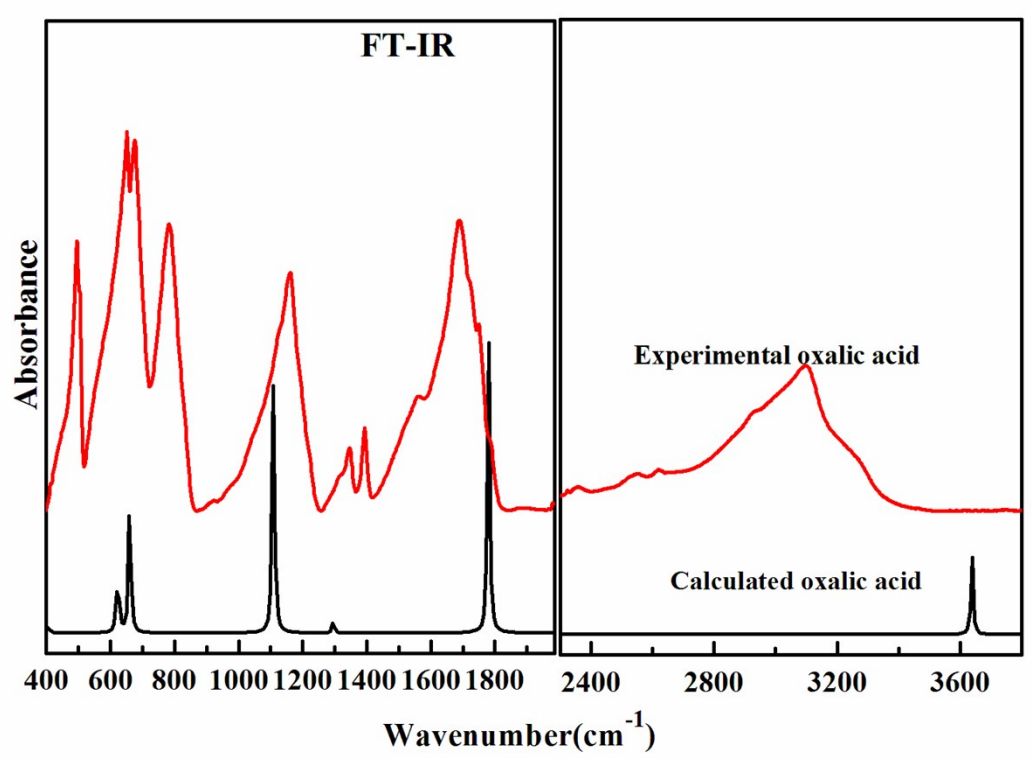

Fig. S7 Experimental and calculated (scaled) IR absorbance spectra of oxalic acid in the region 400-1900cm^{-1} and 2300-3800cm^{-1}

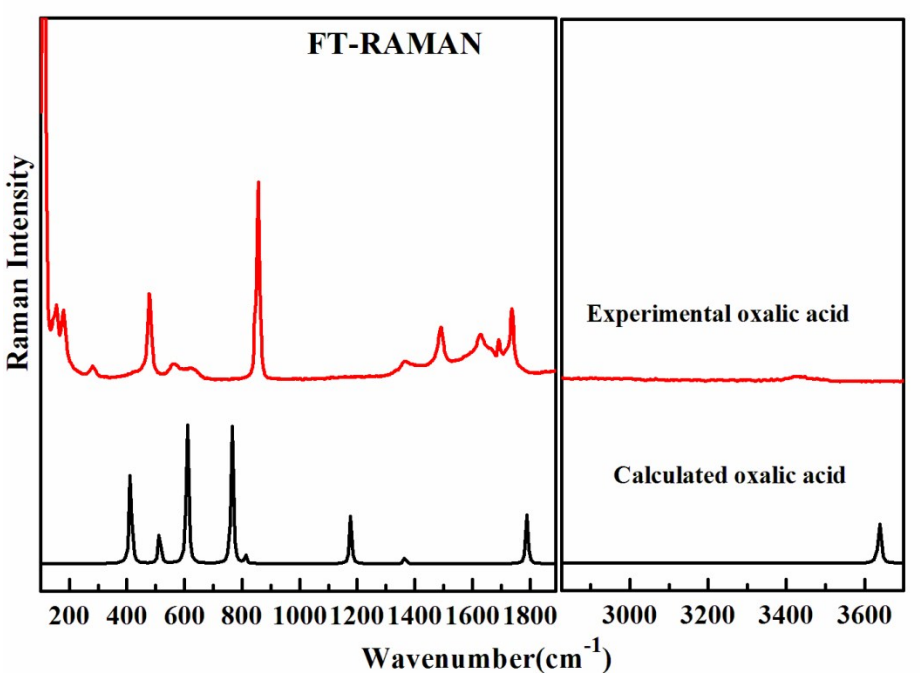

Fig. S8 Experimental and calculated (scaled) Raman scattering spectra of oxalic acid in the region 100-1900cm^{-1} and 2700-3700cm^{-1}.

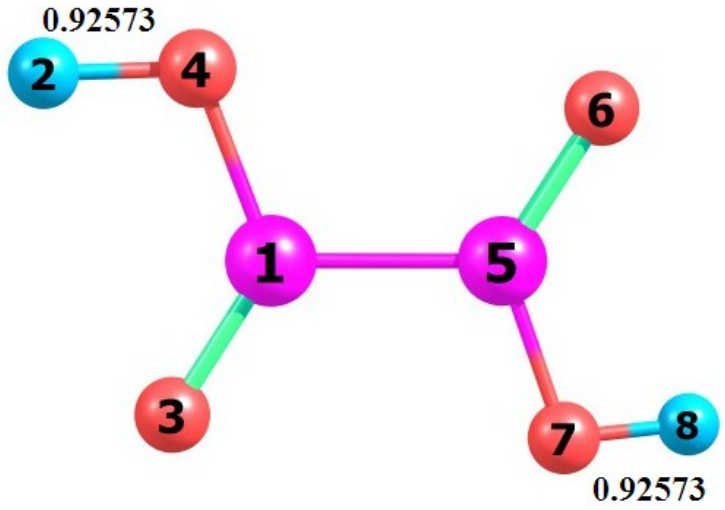

Fig.S9 Experimental structure of oxalic acid

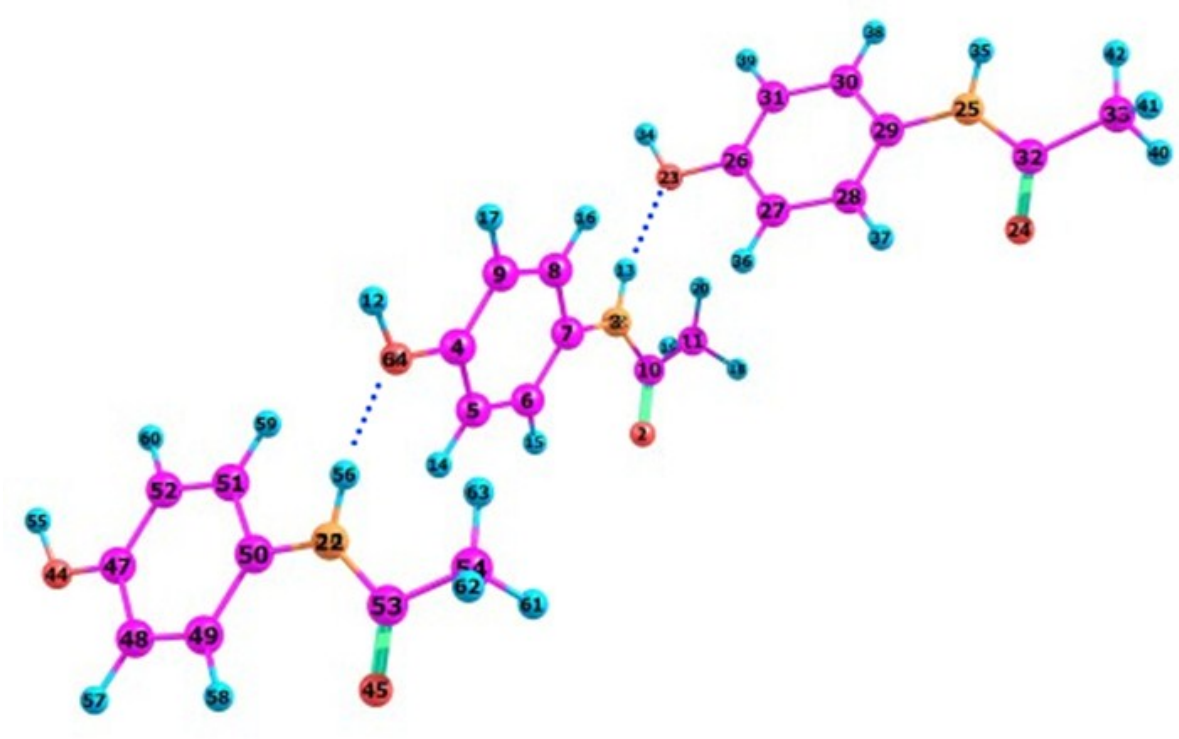

Fig. S10 Experimental structure of paracetamol forming hydrogen bond with neighboring molecule.

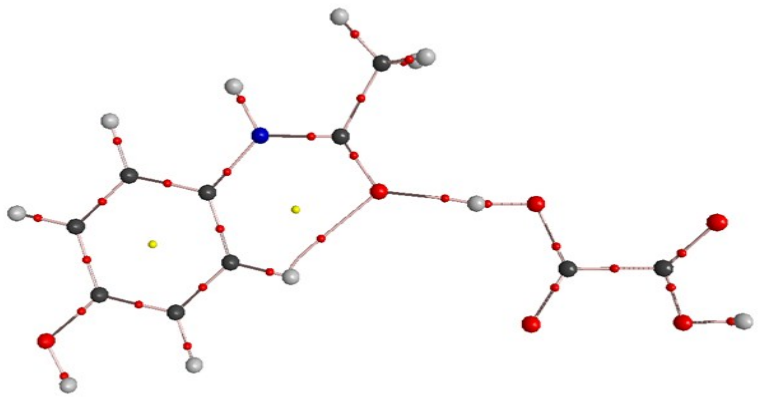

Fig. S11 Molecular graph of monomer of cocrystal: bond critical points (small red spheres), ring critical points (small yellow sphere), bond paths (pink lines).

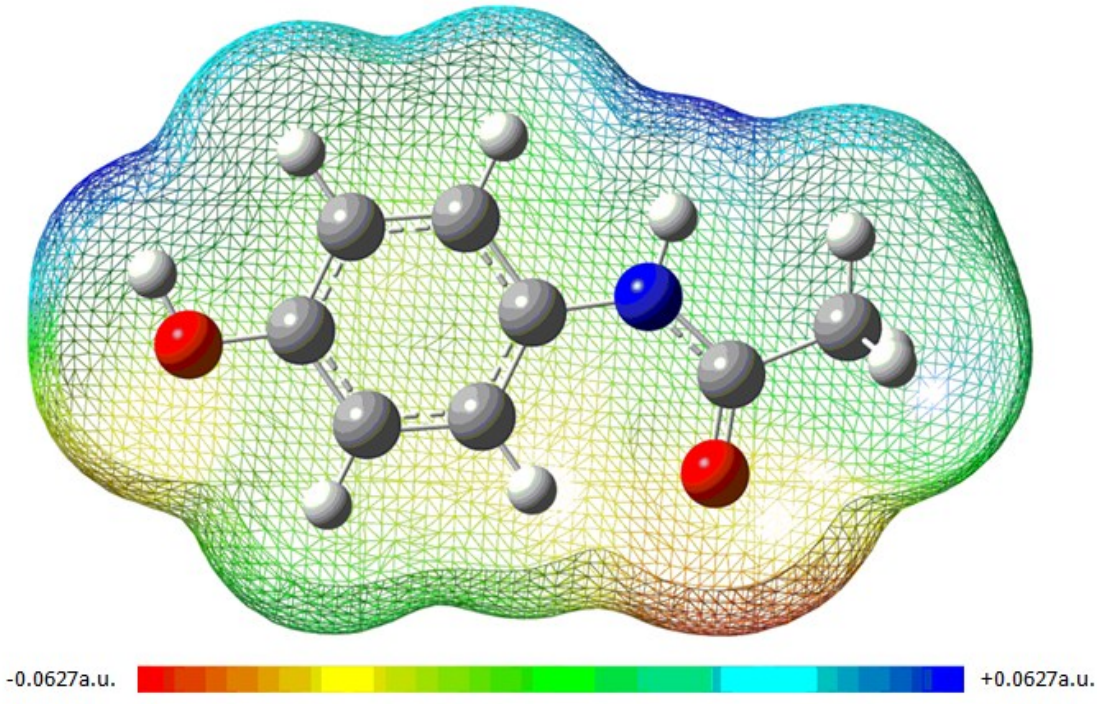

Fig. S12 Molecular electrostatic potential (MEP) formed by mapping of total density over electrostatic potential in gas phase for paracetamol (monomer).

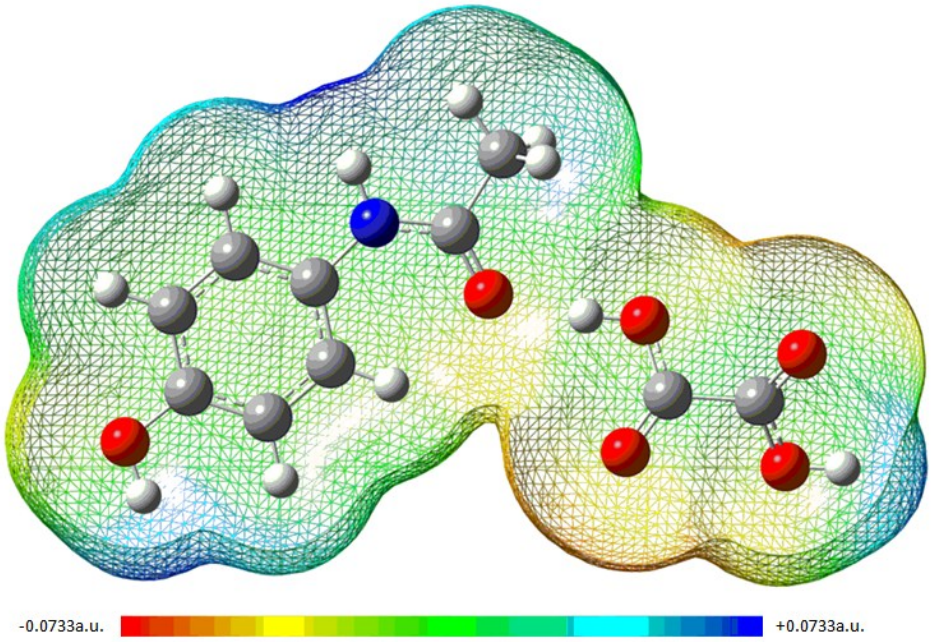

Fig. S13 Molecular electrostatic potential (MEP) formed by mapping of total density over electrostatic potential in gas phase for monomer of cocrystal.

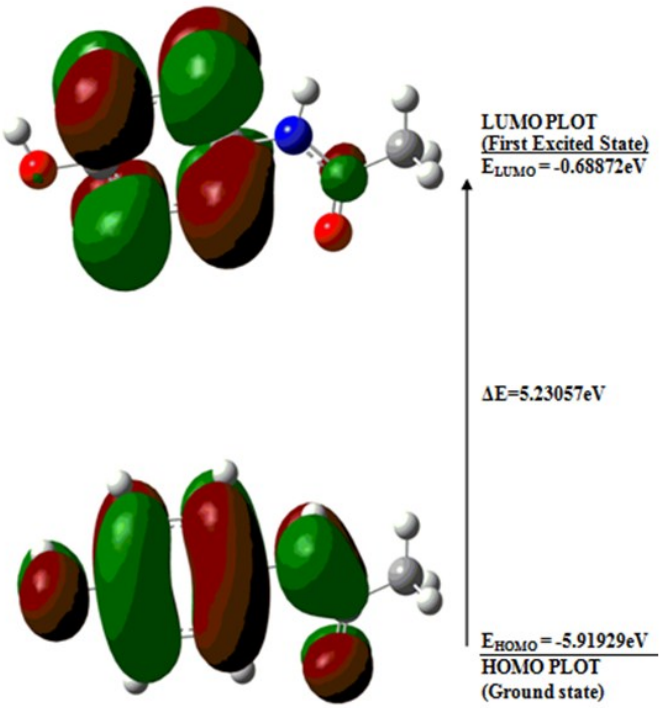

Fig. S14 HOMO-LUMO plot of paracetamol (monomer) with orbitals involved in electronic transitions.

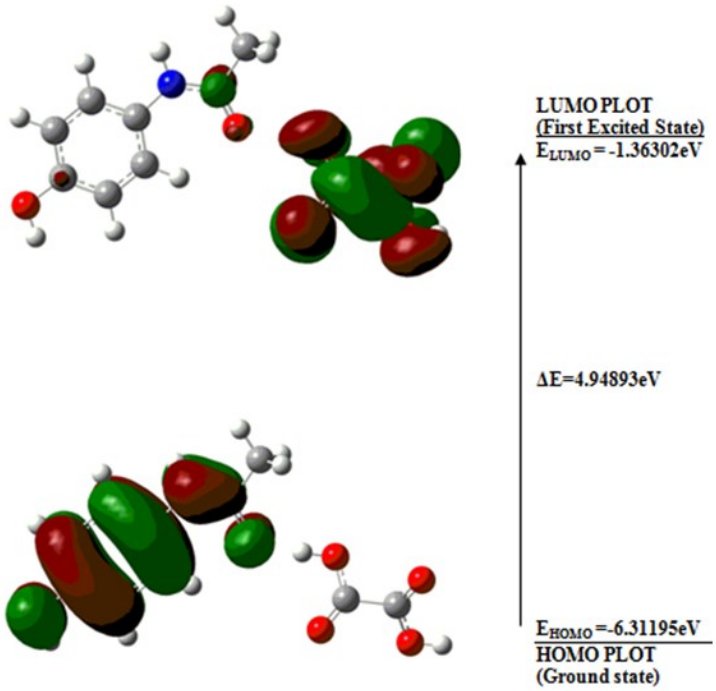

Fig.S15 HOMO-LUMO plot of monomer of cocrystal with orbitals involved in electronic transitions.

Table S1 The experimental and calculated geometric parameters of PRA-OXA cocrystal and calculated geometric parameters of, monomer and dimer+2OXA of cocrystal using DFT/6−311++g(d,p), bond lengths in angstrom (Å) and bond angles in degrees (º).

Geometrical parameters	Experimental	Calculated optimized parameter B3LYP/6−311++G(d, p)	
		Monomer	Dimer+2OXA
Bond length (Å)			
R(C1−C2)	1.39345	1.39759	1.39816
R(C1−C6)	1.39922	1.40103	1.40041
R(C1−N8)	1.41876	1.42109	1.42187
R(C2−C3)	1.39354	1.39320	1.39248
R(C2−H12)	1.08263	1.07865	1.07845
R(C3−C4)	1.39107	1.39363	1.39371
R(C3−H13)	1.08302	1.08587	1.08347
R(C4−C5)	1.39057	1.39565	1.39398
R(C4−O7)	1.36954	1.36815	1.37584
R(C5−C6)	1.39240	1.38668	1.38861
R(C5−H14)	1.08272	1.08286	1.08362
R(C6−H15)	1.08228	1.08598	1.08402
R(O7−H16)	0.98495	0.96295	0.98408
R(N8−C9)	1.35692	1.35865	1.35107
R(N8−H17)	1.00943	1.00862	1.01364
R(C9=O10)	1.24257	1.23288	1.24166
R(C9−C11)	1.51196	1.51396	1.51315
R(O10−H28)	1.58416	1.66421	1.57845
R(C11−H18)	1.08355	1.09216	1.09310
R(C11−H19)	1.08772	1.09124	1.08942
R(C11−H20)	1.08461	1.09218	1.09192
R(C21−O22)	1.28968	1.34362	1.34518
R(C21=O23)	1.23920	1.20147	1.19873
R(C21−C24)	1.55398	1.54056	1.54802
R(O22−H27)	0.98235	0.96977	0.96965
R(C24−O25)	1.26911	1.32208	1.30614
R(C24=O26)	1.23211	1.20415	1.21194
R(O25−H28)	0.98274	0.99878	1.01628
Bond Angle (◦)			
A(C2−C1−C6)	119.19623	119.16810	119.17390
A(C2−C1−N8)	124.12101	123.75666	123.85682
A(C6−C1−N8)	116.68277	117.07310	116.96217
A(C1−C2−C3)	119.75401	119.62335	119.97180
A(C1−C2−H12)	120.37954	120.15897	120.00621
A(C3−C2−H12)	119.80629	120.21726	120.02101
A(C2−C3−C4)	120.85161	120.95516	120.43128
A(C2−C3−H13)	118.90043	118.97009	119.85479
A(C4−C3−H13)	120.19692	120.07463	119.71373
A(C3−C4−C5)	119.57150	119.49810	119.89520
A(C3−C4−O7)	118.40987	123.06122	121.79388
A(C5−C4−O7)	121.99260	117.44067	118.31015
A(C4−C5−C6)	119.74932	119.70837	119.69361
A(C4−C5−H14)	120.06460	119.34320	119.79323
A(C6−C5−H14)	120.16229	120.94833	120.51287
A(C1−C6−C5)	120.81489	121.04654	120.83201
A(C1−C6−H15)	118.95464	119.87807	119.66832
A(C5−C6−H15)	120.23017	119.07539	119.49635
A(C4−O7−H16)	112.20300	109.86848	111.51118
A(C1−N8−C9)	128.60608	129.44713	129.26677
A(C1−N8−H17)	115.50968	114.69869	114.83304
A(C9−N8−H17)	115.78816	115.84912	115.89238
A(N8−C9=O10)	123.45829	122.65767	123.02144
A(N8−C9−C11)	115.19230	115.86705	115.94652
A(O10=C9−C11)	121.34303	121.47520	121.03093
A(C9=O10−H28)	117.58750	129.40171	124.18935
A(C9−C11−H18)	109.60459	108.77933	108.77644
A(C9−C11−H19)	113.59575	113.70092	113.14174
A(C9−C11−H20)	109.36920	108.82200	108.94270
A(H18−C11−H19)	114.82530	109.02587	109.19746
A(H18−C11−H20)	103.44920	107.32092	107.23214
A(H19−C11−H20)	105.29413	109.00028	109.37861
A(O22−C21=O23)	125.33281	124.54287	124.66177

A(O22−C21−C24)	114.90630	111.06988	110.64189
A(O23=C21−C24)	119.40555	124.33810	124.69170
A(C21−O22−H27)	116.25246	107.24056	107.25974
A(C21−C24−O25)	114.96266	110.72880	111.05156
A(C21−C24=O26)	119.45463	122.05010	121.84885
A(O25−C24=O26)	125.40901	127.18046	127.09517
A(C24−O25−H28)	116.26379	111.31885	113.11891
A(O10−H28−O25)	157.32087	172.30292	171.64399
Dihedral Angle (◦)			
D(C6−C1−C2−C3)	2.19375	0.14143	0.33627
D(C6−C1−C2−H12)	179.36761	179.90327	179.97605
D(N8−C1−C2−C3)	−177.79228	179.59227	179.33617
D(N8−C1−C2−H12)	−0.61843	−0.64589	−1.02405
D(C2−C1−C6−C5)	−0.27176	0.03685	−0.12236
D(C2−C1−C6−H15)	179.92799	−179.93848	−179.45605
D(N8−C1−C6−C5)	179.71530	−179.45039	−179.19057
D(N8−C1−C6−H15)	−0.08495	0.57428	1.47574
D(C2−C1−N8−C9)	3.82431	6.08759	11.48121
D(C2−C1−N8−H17)	−172.42649	−174.77475	−169.58932
D(C6−C1−N8−C9)	−176.16204	−174.45094	−169.49850
D(C6−C1−N8−H17)	7.58716	4.68672	9.43096
D(C1−C2−C3−C4)	−3.09673	−0.20458	−0.12594
D(C1−C2−C3−H13)	179.49654	179.92541	179.71176
D(H12−C2−C3−C4)	179.71306	−179.96628	−179.76566
D(H12−C2−C3−H13)	2.30633	0.16371	0.07204
D(C2−C3−C4−C5)	2.02029	0.08717	−0.30271
D(C2−C3−C4−O7)	−179.79822	−179.93679	−179.97888
D(H13−C3−C4−C5)	179.39351	179.95574	179.85936
D(H13−C3−C4−O7)	−2.42500	−0.06821	0.18319
D(C3−C4−C5−C6)	−0.06896	0.09213	0.51490
D(C3−C4−C5−H14)	178.15980	179.98109	−179.67805
D(O7−C4−C5−C6)	−178.18299	−179.88525	−179.79773
D(O7−C4−C5−H14)	0.04577	0.00371	0.00932
D(C3−C4−O7−H16)	0.51489	0.67742	−5.71781
D(C5−C4−O7−H16)	178.65000	−179.34608	174.60107
D(C4−C5−C6−C1)	−0.79675	−0.15436	−0.30342
D(C4−C5−C6−H15)	179.00096	179.82116	179.03140
D(H14−C5−C6−C1)	−179.02375	179.95850	179.89095
D(H14−C5−C6−H15)	0.77396	−0.06598	−0.77423
D(C1−N8−C9=O10)	2.63166	−0.21810	−0.57864
D(C1−N8−C9−C11)	−176.45874	179.88564	179.04086
D(H17−N8−C9=O10)	178.87369	−179.34754	−179.49868
D(H17−N8−C9−C11)	−0.21671	0.75619	0.12081
D(N8−C9=O10−H28)	170.23136	−175.45977	−177.43549
D(C11−C9=O10−H28)	−10.73237	4.43078	2.96381
D(N8−C9−C11−H18)	−114.63612	−121.69396	−115.73288
D(N8−C9−C11−H19)	15.29970	−0.00491	5.80090
D(N8−C9−C11−H20)	132.60080	121.68231	127.68426
D(O10=C9−C11−H18)	66.25241	58.40845	63.89480
D(O10=C9−C11−H19)	−163.81176	−179.90251	−174.57142
D(O10=C9−C11−H20)	−46.51066	−58.21528	−52.68806
D(C9=O10−H28−O25)	70.45775	−13.49524	23.87521
D(O23=C21−O22−H27)	6.11962	0.25686	0.17743
D(C24−C21−O22−H27)	−166.95836	−177.28323	179.42308
D(O22−C21−C24−O25)	176.18445	−139.74951	169.26847
D(O22−C21−C24=O26)	−8.34761	42.41383	−11.44516
D(O23=C21−C24−O25)	2.66465	42.70438	−11.48615
D(O23=C21−C24=O26)	178.13259	−135.13228	167.80022
D(C21−C24−O25−H28)	169.66727	−176.79335	179.66533
D(O26=C24−O25−H28)	−5.49018	0.90517	0.42532
D(C24−O25−H28−O10)	110.49743	170.53534	172.75941

Table S2 Theoretical and experimental vibrational wave numbers (cm^{-1}) of paracetamol

Unscaled	Scaled	IR	Raman	Assignment(% PED)
3838	3715	3321	-	[ν(O1H12)](100)
3628	3512	3256	-	[ν(N3H13)](100)

3243	3139	3107	3104	R1[ν(CH)](98)
3192	3090	-	-	R1[ν(CH)](98)
3165	3063	-	3065	R1[ν(CH)](99)
3148	3047	3036	-	R1[ν(CH)](99)
3115	3015		3010	$\nu_a(CH_3)$](100)
3114	3014	-		$\nu_a(CH_3)$](100)
3041	2943	2931	2931	$\nu_s(CH_3)$](100)
1746	1690	1651	1649	[ν(O2=C10)](75)
1660	1607	1609	1611	R1[ν(CC)(62) +δ_a(10)+δ_{in}(CH)(12)]
1637	1585	1562	1562	R1[ν(CC)(57)+$\delta_{a'}$(7)]+[ρ(N3H13)](7)
1558	1508	1504	1507	[ρ(N3H13)](40)+[ν(N3C10)](15)+R1[ν(N3C7)(9)+δin(CH)(7)+ν(CC)(7)]
1539	1489			R1[δin(CH)(48)+ν(CC)(34)+ν(O1C4)](7)]+[ρ(N3H13)](5)
1490	1442	1435	1446	[$\delta_a(CH_3)$](81)+[$\delta_{sym}(CH_3)$](6)+[ρ'(CH_3)](5)
1470	1423			[$\delta_{a'}(CH_3)$](91) +[ρ(CH_3)](7)
1452	1406	-	-	R1[ν(CC)(32)+δ_{in}(CH)(24)+δ(C4H12O1)(6)]+[ρ(N3H13)](8) +[ν(N3C10)](5)
1400	1355	1369	1372	[$\delta_{sym}(CH_3)$](85) +[$\delta_a(CH_3)$](6)+ [ν(C10C11)](7)
1362	1318	1327	1324	R1[δ(C4H12O1)(14) +δ_{in}(CH)(26) +ν(CC)(55)]
1335	1293	1280	1278	R1[δ_{in}(CH)(37)+ν(CC)(31)+ν(N3C7)(8)]+ [ν(N3C10)](7)
1283	1242	1240	1257	R1[ν(O1C4)(36)+ν(CC)(32)]+ [ρ(N3H13)](6)
1260	1219	1225	1238	R1[ν(N3C7)(14)+δ_{tri}(13)+ν(O1C4)(12)+δ_{in}(CH)(16)+ν(CC)(6)]+[ν(N3C10)](9)+[ρ(N3H13)](12)
1234	1195	1171	1169	R1[ν(N3C7)(18)+δ_{tri}(6)]+[ν(N3C10)](16)+[ν(C10C11)](13)+[δ_{sci}(C10C11)](7)+[ρ(C10C11)](6)+[ρ'(CH_3)](5)
1197	1158			R1[δ_{in}(CH)(78)+ν(CC)(5)]
1187	1149	1124	1124	R1[δ(C4H12O1)(50)+ν(CC)(22)+δ_{in}(CH)(13)+ν(O1C4)(6)]
1133	1097	1107	1106	R1[δ_{in}(CH)(56)+ν(CC)(23)+δ(C4H12O1)(5)]
1050	1016	1030	1036	[ρ(CH_3)](55)+[ρ'(CH_3)](19)+[ω(C10C11)](16)+[δa'(CH_3)](9)
1027	994	1014	1017	R1[δ_{tri}(41)+ν(CC)(38)+δ_{in}(CH)(5)]
1013	980	-	-	[ρ'(CH_3)](45)+[ρ(CH_3)](15)+[ν(C10C11)](8)+[ν(N3C10)](7) +R1[δ_{tri}](7)
985	953	968	969	R1[δ_{out}(CH)(87)+puck(6)+$\tau_{a'}$(5)]
964	933	924	949	[ν(C10C11)](29)+[δ_{sci}(C10C11)](17)+[δ_{sci}(N3H13)](16)+[ν(N3C10)](16)+R1[ν(CC)](6)
909	879	856	859	R1[δ_{out}(CH)(79)+puck(13)]
863	836	835	835	R1[ν(CC)(46)+δ_a(15)+ν(N3C7)](10)+ν(O1C4)(8)]+[δ_{sci}(N3H13)](6)
855	827	806	824	R1[δ_{out}(CH)](75)+δ_{out}(C4O1)(8)+τ_a(8)]
801	776	796	798	R1[δ_{tri}(24)+ν(O1C4)(17)+ν(CC)(6)+ν(N3C7)(6)+[δ_{sci}(N3H13)](12)+[ν(C10C11)](9)+[δ_{sci}(C10C11)](6)
797	772			R1[δ_{out}(CH)(82)+τ_a(6)+ δ_{out} (C7N3)(5)]
705	682	683	689	R1[puck(65)+δ_{out}(C7N3)(14)+δ_{out}(C4O1)(14)]
657	636	625	628	R1[$\delta_{a'}$(64)+δ_{in}(C4O1)(6)+δ_{in}(C7N3)(5)]
629	609	602	605	[ν(C10C11)](18)+[δ_{sci}(C10C11)](18)+R1[$\delta_{a'}$(14)+δ_a(14)+ν(N3C7)(6)]+[δ_{sci}(N3H13)](8)
627	607	-	-	[ω(C10C11)](60)+[τ(N3C10)](14)+[ρ(CH_3)](12)
527	510	517	518	[ω(N3H13)](46)+[τ(N3C10)](21)+ [ω(C10C11)](17)
521	504	501	505	R1[δ_{out}(C4O1)(32)+τ_a(31)+δ_{out}(C7N3)(26)]
507	491	462	466	[ρ(C10C11)](38)+R1[δ_a](33)+[δ_{sci}(C10C11)](8) +[ρ'(CH3)](6)
429	415	413	412	R1[δ_{in}(C4O1)(51)+$\delta_{a'}$(17)+δ_{in}(C7N3)(16)]+[δ_{sci}(C10C11)](7)
421	407		393	R1[$\tau_{a'}$(82) +[δ_{out}(CH)(12)]
375	363	-		R1[puck(34)+δ_{out}(C4O1)(19)+δ_{out}(C7N3)(18)+δ_{out}(CH)(5)]+ [τ(N3C10)](6)
326	316	-	331	[ρ(C10C11)](29)+[δ_{sci}(C10C11)](14) +R1[δ_{in}(C7N3)(14)+δ_a(12) +δ_{in}(C4O1)(9)+ν(N3C7)(7)]
313	303	-	-	R1[δ_{in}(C7N3)(23)+δ_{in}(C4O1)(10)+δ_a(8)+ν(N3C7)(5)+ν(CC)(5)+[δ_{sci}(N3H13)](19)+[δ_{sci}(C10C11)](10)+[ν(N3C10)](9)
263	255	-		R1[τ(C4O1)(89)+$\tau_{a'}$(5)]
183	177	-	215	R1[τ_a(55)+[δ_{out}(CH)(6)]+ [τ(N3C10)](14)+[ω(N3H13)](11)
155	150	-	154	[δ_{sci}(N3H13)](45)+R1[δ_{in}(C7N3)](33)+[ρ(C10C11)](9)
79.3	76.7	-	-	[τ(C10C11)](28)+R1[τ_a(25)+δ_{out}(C7N3)(10)]+[ω(N3H13)](14)+[τ(N3C10)](9)
46.6	45.1	-	-	[τ(C10C11)](52)+[τ(N3C10)](21)+[ω(C10C11)](15)
41.5	40.2	--	-	R1[τ(C7N3)](70)+[ω(N3H13)](14)+[τ(C10C11)](7)

Table S3 Theoretical and experimental vibrational wave numbers (cm^{-1}) of oxalic acid

Unscaled	scaled	IR	Raman	Assignment(%PED)
3759	3638	3099	-	[υ(O7H8)](50) +[υ(O4H2)](50)

3758	3638		-	[υ(O4H2)](50) +[υ(O7H8)](50)
1849	1790	1749	1739	[υ(C1=O3)](37) +[υ(C5=O6)](37) +[υ(C1C5)](6)
1839	1780			[υ(C5=O6)](44)+[υ(C1=O3)](44)
1411	1366	1394	1369	[υ(C1C5)](20)+[υ(C1O4)](17)+[υ(C5O7)](17)+[δ_{sci}(C1O4)]](10)+[δ_{sci}(C5O7)](10)+[δ(C1H2O4)](10) +[δ(C5H8O7)](10)
1338	1295	1346	-	[δ(C5H8O7)](32)+[δ(C1H2O4)](32) + [υ(C5O7)](10) +[υ(C1O4)](10) +[ρ(C5O7)](6)+[ρ(C1O4)](6)
1216	1177	1161	-	[δ(C1H2O4)](27)+[δ(C5H8O7)](27)+[υ(C1O4)](15)+[υ(C5O7)](15)+ [υ(C1C5)](5)
1145	1109	-	-	[υ(C5O7)](32)+[υ(C1O4)](32)+[δ(C5H8O7)](14)+[δ(C1H2O4)](14)
839	812	785	-	[ω(C5O7)](48) +[ω(C1O4)](48)
791	765		-	[υ(C1C5)](38)+[ρ(C5O7)](12)+[ρ(C1O4)](12)+[υ(C1O4)](12) +[υ(C5O7)](12) +[δ(C5H8O7)](5) + [δ(C1H2O4)](5)
682	660	675		[τ(C1O4)](41)+[τ(C5O7)](41)+[ω(C1O4)](9)+[ω(C5O7)](9)
644	623	652	620	[ρ(C1O4)](30)+[ρ(C5O7)](30)+[δ_{sci}(C1O4)](11) +[δ_{sci}(C5O7)](11)+ [δ(C1H2O4)](7)+[δ(C5H8O7)](7)
630	610	-	603	[τ(C5O7)](49) +[τ(C1O4)](49)
531	514	494	479	[δ_{sci}(C5O7)](29)+[δ_{sci}(C1O4)](29)+[ρ(C1O4)](12)+[ρ(C5O7)](12)+ [υ(C1C5)](7)
427	413	-	-	[υ(C1C5)](35)+[ρ(C1O4)](27) +[ρ(C5O7)](27)
419	406	-	-	[ω(C1O4)](42)+[ω(C5O7)](42)+[τ(C1O4)](8) +[τ(C5O7)](8)
264	255	-	281	[δ_{sci}(C1O4)](35)+[δ_{sci}(C5O7)](35)+[ρ(C1O4)](15)+[ρ(C5O7)](15)
33	31.8	-	-	[τ(C1C5)](84)+[ω(C1O4)](7)+[ω(C5O7)](7)

Table S4 Experimental and theoretical vibrational wave numbers (cm^{-1}) of cocrystal with potential energy distribution (PED).

Frequency(cm^{-1})	monomer				dimer+2OX A	
Calculated		Experimental		Potential Energy Distribution (≥5%)	Calc. Scaled Freq.(cm^{-1})	Simplified description of modes of dimer+2OXA
Unscaled DFT	Scaled	IR	Raman			
3836	3712	3383	3380	[ν(O7H16)](100)	3713,3320	OH stretch
3751	3631	-	-	[ν(O22H27)](100)	3636,3631	OH stretch
3625	3509	3344	3346	[ν(N8H17)](99)	3439,3421	NH stretch
3245	3141	3155	3157	R1[ν(CH)](99)	3144,3141	Ring CH stretch
3198	3095			R1[ν(CH)](96)	3091,3090	Ring CH stretch
3189	3086	2999	-	[ν(O25H28)](93)+[ν(O10H28)](6)	2849,2777	OH stretch
3158	3057	3051	3055	R1[ν(CH)](95)	3089,3076	Ring CH stretch
3153	3052			R1[ν(CH)](93)	3071,3052	Ring CH stretch
3122	3022	3024	3020	[$\nu_a(CH_3)$](100)	3050,3039	CH_3asym stretch
3114	3014			[$\nu_a(CH_3)$](100)	3013,3009	CH_3asym stretch
3045	2947	2945	2941	[$\nu_s(CH_3)$](100)	2950,2948	CH_3 sym stretch
1822	1764	1724	1749	[ν(C21=O23)](70)+[ν(C24=O26)](7)+[ν(C21C24)](6)+[ρ(C21O22)](5)	1773,1690	C=O stretch
1804	1746			[ν(C24=O26)](71)+[ν(C24O25)](8)+[ν(C21=O23)](8)	1754,1721	C=O stretch
1697	1643	1655	-	[ν(C9=O10)](68)+[ρ(N8H17)](6)+[ν(N8C9)](5)+[ρ(C9C11)](5)	1623,1616	C=O stretch
1656	1603	1620	1618	R1[ν(CC)(57)+δ_a(11)+δ_{in}(CH)(11)]	1604,1603	Ring CC stretch
1644	1591	1562	1573	R1[ν(CC)(59)+$\delta_{a'}$(7)+δ_{in}(C1N8)(5)]+ρ(N8H17)](9)	1597,1596	Ring CC stretch
1572	1521	1514	1519	[ρ(N8H17)](39)+[ν(N8C9)](22)+R1[ν(C1N8)(6)+ν(CC)(5)]	1550,1548	NH rocking
1542	1493	1470	-	R1[δ_{in}(CH)(48)+ν(CC)(35)+ν(C1N8)(7)+ν(C4O7)(7)]	1497,1495	In plane ring def
1492	1444	1446	1444	[$\delta_{a'}(CH_3)$](55)+[$\delta_a(CH_3)$](18)+[$\delta_{sym}(CH_3)$](9)+[ρ'(CH_3)](5)	1451,1444	CH_3asymdef
1472	1424	1431	1420	[$\delta_a(CH_3)$](67)+[$\delta_{a'}(CH_3)$](23)+[ρ(C11H3)](7)	1434,1432	CH_3asymdef
1457	1410	1402	-	R1[ν(CC)(31)+δ_{in}(CH)(28)+δ(C4H16O7)(6)]+[ν(N8C9)](5)	1421,1415	Ring CC stretch
1439	1392	1383	1385	[δ(C24H28O25)](46)+[ν(C24O25)](16)+[ν(C21C24)](11)+[δ_{sci}(C24O25)](7)+ [ν(C21O22)](5)	1411,1408	CHO def
1408	1363	1358	1361	[$\delta_{sym}(CH_3)$](81)+[$\delta_{a'}(CH_3)$](7)+[ν(C9C11)](7)	1368,1365	sym CH_3 def
1364	1320	1323	1334	R1[δ(C4H16O7)(12)+ν(CC)(61)+δ_{in}(CH)(17)]	1359,1323	Ring CC stretch
1359	1316			[δ(C24H28O25)](25)+[δ(C21H27O22)](20)+[ν(C21O22)](17)+[ν(C21C24)](7)+[δ_{sci}(C21O22)](7)	1335,1325	CHO def
1347	1304	1300	1280	R1[δ_{in}(CH)(37)+ν(CC)(7)+ν(C1N8)(7)]+[ν(N8C9)](9)	1313,1312	Ring in plane CH deformation
1290	1248	-	1247	R1[ν(C4O7)(27)+ν(CC)(17)+δ_{in}(CH)(15)]+[ρ(N8H17)](9)	1245,1233	Ring CO stretch
1273	1233	1221	1223	R1[ν(C4O7)](19)+ν(CC)(16)]+[ρ(N8H17)](12)+[ν(N8C9)](11)+[ν(C9C11)](5)	1226,1220	Ring CO stretch+N8C9 stretch
1257	1217			[ν(C24O25)](35)+[δ(C21H27O22)](22)+[δ(C24H28O25)](19)	1248,1245	CO stretch
1239	1199	1178	1182	R1[ν(C1N8)(37)+δ_{tri}(14)+ν(CC)(15)+δ_{in}(CH)(10)]+[ν(C9C11)(6)	1204,1200	Ring CN stretch

1198	1159	-	-	R1[δ_{in}(CH)(68)+δ(C4H16O7)(11)+ν(CC)(12)]	1172,1163	Ring CH in plane deformation
1188	1150	1128	1128	R1[δ(C4H16O7)(42)+ν(CC)(16)+δ_{in}(CH)(16)+ν(C4O7)(7)]	1160,1149	Ring CHO deformation
1154	1117	1115	1116	[ν(C21O22)](46)+[δ(C21H27O22)](26)+[ν(C24O25)](14)	1127,1123	CO stretching
1134	1098			R1[δ_{in}(CH)(56)+ν(CC)(22)+δ(C4H16O7)(5)]	1107,1098	In plane CH deformation
1055	1021	1022	1030	[ρ(CH_3)](55)+[ρ'(CH_3)](18)+[ω(C9C11)](16)+[δ_a(CH_3)](8)	1029,1020	CH_3 rocking
1031	998			[ρ'(CH_3)](35)+[ρ(CH_3)](10)+R1[δ_{tri}(10)+ν(C1C2)(13)]	1012,1008	CH_3 rocking
1024	991	970	971	R1[δ_{tri}(37)+ν(CC)(14)]+[ρ'(CH_3)](18)+[ρ(CH_3)](6)	998,995	Ring tri deformation
979	948	-	-	[ν(C9C11)](19)+[τ(O25H28)](13)+[δ_{sci}(C9C11)](12)+[δ_{sci}(N8H17)](10)+[ν(N8C9)](9)+[τ(C24O25)](9)+R1[δ_{out}(CH)](8)	947,944	C9C11 stretching
975	943	937	-	[τ(O25H28)](21)+R1[δ_{out}(CH)](23)+[τ(C24O25)](14)+[ν(C9C11)](11)+[δ_{sci}(C9C11)](7)+[δ_{sci}(N8H17)](6)	962,942	O25H28 torsion
971	939			R1[δ_{out}(CH)(65)+$\tau_{a'}$(5)]+[τ(O25H28)](12)+[τ(C24O25)](7)	957,942	Ring out of plane CH deformation
940	910	-	-	R1[δ_{out}(CH)(78)+puck(15)]	924,922	Ring out of plane CH deformation
867	839	837	841	R1[ν(CC)(44)+δ_a(15)+ν(C1N8)(11)+ν(C4O7)(7)]+[δ_{sci}(N8H17)](7)	841,841	Ring CC stretching
841	814	823	828	R1[δ_{out}(CH)(69)+δ_{out}(C4O7)(12)+τ_a(11)+δ_{out}(C1N8)(6)]	833,817	Ring out of plane CH deformation
837	810	796	798	[ω(C21O22)](44)+[ω(C24O25)](42)	813,811	CO wagging
816	790			R1[δ_{out}(CH)](96)	805,794	Ring out of plane CH deformation
812	786	-	-	[ν(C21C24)](33)+[ρ(C24O25)](19)+[ν(C24O25)](13)+[ν(C21O22)](12)+[ρ(C21O22)](6)+[δ(C24O25O10)](6)	797,797	CC stretching
805	780	-	-	R1[δ_{tri}(24)+ν(C4O7)(17)+ν(CC)(11)+ν(C1N8)(5)]+[δ_{sci}(N8H17)](12)+[ν(C9C11)](9)+[δ_{sci}(C9C11)](6)	781,780	Ring tri deformation
712	689	696	709	R1[puck(66)+δ_{out}(C1N8)(14)+δ_{out}(C4O7)(14)]	700,693	Ring puckering
697	675	656	656	[τ(C21O22)](25)+[ω(C24O25)](24)+[ω(C21O22)](18)+[δ_{sci}(C21O22)](11)+[ρ(C24O25)](7)+[δ_{sci}(C24O25)](5)	662,656	CO torsion
664	643		633	[ρ(C21O22)](29)+[ρ(C24O25)](22)+[δ(C21H27O22)](7)+[δ_{sci}(C24O25)](7) +[δ_{sci}(C21O22)](6)	653,649	CO rocking
658	637	-		R1[$\delta_{a'}$(56)+δ_{in}(C4O7)(5)]	639,638	Ring asym deformation
633	613	611	615	[ω(C9C11)](19)+[δ_{sci}(C9C11)](11)+[ν(C9C11)](10)+R1[$\delta_{a'}$(9)+δ_a(7)+ [τ(N8C9)](8)	618,615	CC wag+ CC scis
631	610			[ω(C9C11)](35)+[τ(N8C9)](13)+[ρ($C11H_3$)](9) +R1[$\delta_{a'}$](6)+[δ_{sci}(C9C11)](6)+[ν(C9C11)](6)	595,594	CC wag+N8C9 torsion
589	571	-	-	[τ(C21O22)](66)+[δ_{sci}(C24O25)](11)+[ρ(C21O22)](6)	557,536	CO tors+ CO scis
559	541	521	524	[ω(N8H17)](46)+[ω(C9C11)](20)+[τ(N8C9)](18)	512,509	NH wagging
522	505	-	-	R1[τ_a(31)+δ_{out}(C4O7)(30)+δ_{out}(C1N8)(27)]	504,503	Ring torsion
514	497	488	471	[ρ(C9C11)](36) +R1[δ_a](32) +[δ_{sci}(C9C11)](6)+[ρ'($C11H_3$)](5)	503,474	CC rocking
441	427	440	440	R1[δ_{in}(C4O7)](26)+δ_{in}(C1N8)(15)+$\delta_{a'}$(12)]+[ν(O10H28)](9)+[ν(C21C24)](9)+[ρ(C21O22)](6)	430,420	In plane ring C4O7 deformation
425	411	415	-	R1[δ_{in}(C4O7)(27)+$\delta_{a'}$(8)+δ_{in}(C1N8)(5)]+[ν(C21C24)](20)+[ρ(C21O22)](12)+ [ρ(C24O25)](9)	420,413,	In plane ring C4O7 deformation
419	406		392	R1[$\tau_{a'}$(82) +δ_{out}(CH)(15)]	410,408	Ring torsion
377	365	-	376	R1[puck(30)+δ_{out}(C1N8)(20)+δ_{out}(C4O7)(19)+δ_{out}(CH)(5)]+[τ(N8C9)](7)	374,369	Ring puckering
359	347	-	343	[ω(C21O22)](17)+[δ_{sci}(C24O25)](16)+[ω(C24O25)](13)+[ν(O10H28)](10)+[δ_{sci}(C21O22)](8)+R1[δ_{in}(C4O7)](7)+ [δ_{sci}(N8H17)](5)	362,347	CC wag+ CC scis
339	328	-	-	R1[δ_{in}(C1N8)(14)+δ_{in}(C4O7)(10)]+[δ_{sci}(N8H17)](10)+[ω(C24O25)](9)+[δ_{sci}(C9C11)](8)+[ω(C21O22)](8)+[δ_{sci}(C21O22)](8)+[ρ(C21O22)](6)+[ρ(C9C11)](5)	323,314	In plane ring C1N8 deformation
324	314	-	-	[ρ(C9C11)](31)+R1[δ_a(25)+ν(C1N8)(15)]+[ν(N8C9)](5)	326,288	C9C11 rocking
303	293	-	-	[τ(C4O7)](89)+ R1[$\tau_{a'}$](5)	282,272	C4O7 torsion
274	265	-	-	[δ_{sci}(C21O22)](26))+[δ_{sci}(C24O25)](26)+[ρ(C21O22)](15)+[δ(C24O25O10)](5) +[ρ(C24O25)](5)	272,261	CO scissoring
191	185	-	212	R1[τ_a](43)+[τ(N8C9)](13)+[ω(N8H17)](9)	214,194	Ring torsion
175	169	-	140	R1[δ_{in}(C1N8)(27)+τ_a(7)]+[ν(O10H28)](14)+[δ_{sci}(N8H17)](13)+[ρ(C9C11)](5)+[ρ(C24O25)](5)	187,146	In plane ring C1N8 deformation
96	92.9	-	-	[δ(C24O25O10)](19)+[δ(C24H28O25)](12)+[τ(C24O25)](10)+[ν(O10H28)](9)+[τ(C9=O10)](8)+[τ(C9C11)](7)+[δ_{sci}(N8H17)](6)+[ρ(C24O25)](6)	101,97.6	COO def+ CHO def
93.7	90.7	-	-	[ν(O10H28)](31)+[τ(C9C11)](21)+[τ(C9=O10)](6)+R1[τ_a](6)+[δ_{sci}(N8H17)](5)	89.2,82.8	OH stre + CC tors
85.9	83.2	-	-	[δ(C24O25O10)](25)+[ν(O10H28)](16)+[τ(C9C11)](15)+R1[τ_a(7)+δ_{out}(C1N8)(5)]+[τ(O10O25)](5)+ [τ(C24O25)](5)	80.4,	COO def

77.2	74.7	-	-	[δ(C24O25O10)](39)+[τ(C24O25)](15)+[δ(C24H28O25)](12)+[ν(O10H28)](11)+[δ(C9O10O25)](7)	75.3,70	COO def
62.8	60.8	-	-	[τ(C9C11)](40)+[τ(N8C9)](25)+[ω(C9C11)](10) +[ω(N8H17)](8)	55,51	CC tors
39.9	38.6	-	-	R1[τ(C1N8)](57)+[τ(O25H28)](22)+[τ(O10O25)](8)	42.2,36.1	Ring C1N8 torsion
21.1	20.4	-	-	[τ(O25H28)](55)+[τ(O10O25)](32)+[τ(C9=O10)](7)	26.2,24.7	OH torsion
17.3	16.7	-	-	[τ(O10O25)](45)+[τ(O25H28)](41)+[τ(C21C24)](6)	13.9,13	OH torsion +OO torsion
11.2	10.8	-	-	[δ(C24O25O10)](28)+[δ(C9O10O25)](26)+[τ(O25H28)](20)+[τ(O10O25)](14)	13,10.4	COO def
7.79	7.54	-	-	[τ(O10O25)](36)+[τ(C21C24)](21)+[τ(O25H28)](16)+[τ(C9=O10)](5)	8.4,5.81	OO torsion+CC torsion

Table S5 Selected Lewis orbitals (occupied bond orbital or lone pair) with percentage ED over bonded atoms (ED_X, ED_Y in %), hybrid NBOs with s and p character in % for monomer of cocrystal.

Bond (X –Y) (ED_X-$_Y$)	ED_X(%) ED_Y(%)	Hybrid NBOs	s(%)	p(%)
σ(C1-N8)	37.71	$0.6141(sp^{2.77})_C$ +	26.51	73.39
1.98663	62.29	$0.7892(sp^{1.76})_N$	36.24	63.73
σ (C4-O7)	32.42	$0.5693(sp^{3.09})_C$+	24.40	75.39
1.99419	67.58	$0.8221(sp^{1.93})_O$	34.08	65.86
σ (O7-H16)	78.11	$0.8838(sp^{2.81})_O$+	26.23	73.70
1.98831	21.89	$0.4678(sp^{0.00})_H$	99.79	0.21
σ (N8-C9)	62.77	$0.7923(sp^{1.71})_N$+	36.86	63.09
1.98898	37.23	$0.6102(sp^{2.11})_C$	32.09	67.80
σ (N8-H17)	71.93	$0.8481(sp^{2.72})_N$ +	26.85	73.11
1.98197	28.07	$0.5298(sp^{0.00})_H$	99.92	0.08
σ (C9-O10)	34.84	$0.5902(sp^{2.18})_C$ +	31.36	68.48
1.99285	65.16	$0.8072(sp^{1.56})_O$	38.97	60.91
σ(C21-O22)	32.18	$0.5673(sp^{2.45})_C$ +	28.95	70.84
1.99563	67.82	$0.8235(sp^{2.00})_O$	33.25	66.65
σ(C21-O23)	35.22	$0.5935(sp^{1.78})_C$ +	35.96	63.88
1.99748	64.78	$0.8048(sp^{1.47})_O$	40.50	59.38
σ (O22-H27)	74.83	$0.8651(sp^{3.69})_O$ +	21.29	78.62
1.98668	25.17	$0.5017(sp^{0.00})_H$	99.84	0.16
σ (C24-O25)	33.26	$0.5767(sp^{2.21})_C$ +	31.11	68.68
1.99506	66.74	$0.8169(sp^{1.88})_O$	34.64	65.27
σ (C24-O26)	34.92	$0.5910(sp^{1.80})_C$ +	35.60	64.25
1.99619	65.08	$0.8067(sp1.46)_O$	40.53	59.36
σ (O25-H28)	79.34	$0.8907(sp^{2.75})_O$ +	26.64	73.29
1.98230	20.66	$0.4545(sp^{0.00})_H$	99.74	0.26
LP(1)(O7) 1.93717	-	$(sp^{1.68})$	37.34	62.64
LP(2)(O7) 1.88141	-	$(sp^{41.73})$	2.34	97.63
LP(1)(N8) 1.62516	-	$(sp^{1.00})$	0.00	99.99
LP(1)(O10) 1.95343	-	$(sp^{0.88})$	53.29	46.69
LP(2)(O10) 1.84964	-	$(sp^{12.79})$	7.25	92.71
LP(1)(O22) 1.97558	-	$(sp^{1.20})$	45.54	54.42
LP(2)(O22) 1.81155	-	$(sp^{1.00})$	0.00	99.94
LP(1)(O23) 1.98178	-	$(sp^{0.68})$	59.50	40.49
LP(2)(O23) 1.83885	-	$(sp^{99.99})$	0.02	99.89
LP(1)(O25) 1.96462	-	$(sp^{1.58})$	38.72	61.24
LP(2)(O25) 1.74774	-	$(sp^{1.00})$	0.00	99.94
LP(1)(O26) 1.97264	-	$(sp^{0.68})$	59.38	40.61
LP(2)(O26) 1.86056	-	$(sp^{99.99})$	0.04	99.89

Table S6 Geometrical parameters for intra and inter molecular hydrogen bonds in dimer+2OXA of cocrystal: bond length (Å), bond angle (◦) and sum of van der Waal radii of interacting atoms ($r_H + r_A$) in Å.

Interactions(D-H…A)	d_{D-H}(A°)	d_{H-A}(A°)	d_{D-A}(A°)	D-H…A(°)	(r_H+r_A)(A°)
O38-H43.....O7	1.0153	1.5272	2.5299	168.4079	2.72
C6-H15....O50	1.0708	2.5445	3.4161	137.9763	2.72
N8-H17....O50	1.0038	1.9533	2.9511	172.2526	2.72
O7-H16....O31	0.9889	1.6183	2.5920	167.2276	2.72
C3-H13....O31	1.0703	2.3542	3.1293	128.0243	2.72
O33-H36....O62	1.0107	1.566	2.5510	163.1701	2.72
C54-H64....O62	1.0649	2.1784	2.8623	119.9039	2.72
N60-H69....O26	1.0053	1.8488	2.8489	172.7244	2.72
C63-H71....O26	1.0757	2.3767	3.3056	143.7022	2.72
O25-H28....O10	1.0214	1.5106	2.5287	173.9701	2.72
C2-H12....O10	1.0632	2.1804	2.8635	119.9527	2.72
C58-H67....O22	1.0725	2.5119	3.5753	171.0310	2.72
C11-H19....O46	1.0789	2.4009	3.4776	175.5575	2.72

Table S7 Reactivity descriptors as Fukui functions ($fk^{+,}$ fk^{-}), local softnesses (sk^{+},sk^{-}), local electrophilicity indices(ωk^{+}, ωk^{-}) for paracetamol(monomer), using Hirshfeld atomic charges.

Sites	f_k^+	s_k^+	ωk^+	**Sites**	f_k^-	s_k^-	ωk^-
1 O	0.103478	0.019125	0.148224	1 O	0.026653	0.004926	0.038178
2 O	0.080495	0.014877	0.115303	2 O	0.02538	0.004691	0.036355
3 N	0.071728	0.013257	0.102745	3 N	0.003046	0.000563	0.004363
4 C	0.085104	0.015729	0.121905	4 C	0.019001	0.003512	0.027217
5 C	0.06468	0.011954	0.092649	5 C	0.019811	0.003661	0.028378
6 C	0.055113	0.010186	0.078945	6 C	0.016157	0.002986	0.023144
7 C	0.07858	0.014523	0.11256	7 C	0.012799	0.002366	0.018334
8 C	0.065102	0.012032	0.093253	8 C	0.037386	0.00691	0.053552
9 C	0.062807	0.011608	0.089966	9 C	0.042254	0.007809	0.060525
10 C	0.035905	0.006636	0.051431	10 C	0.01853	0.003425	0.026543
11 C	0.019202	0.003549	0.027505	11 C	0.058579	0.010827	0.08391
12 H	0.041118	0.007599	0.058898	12 H	0.147137	0.027194	0.210762
13 H	0.033156	0.006128	0.047493	13 H	0.092852	0.017161	0.133003
14 H	0.037902	0.007005	0.054292	14 H	0.016404	0.003032	0.023497
15 H	0.029468	0.005446	0.042211	15 H	0.011349	0.002098	0.016257
16 H	0.037002	0.006839	0.053002	16 H	0.110499	0.020422	0.158281
17 H	0.03813	0.007047	0.054618	17 H	0.118031	0.021814	0.16907
18 H	0.023017	0.004254	0.03297	18 H	0.046405	0.008577	0.066471
19 H	0.023017	0.004254	0.03297	19 H	0.046398	0.008575	0.066461
20 H	0.015026	0.002777	0.021524	20 H	0.118481	0.021898	0.169715

TableS8 Reactivity descriptors as Fukui functions (fk+, fk-), local softnesses (sk+,sk-), local electrophilicity indices (ωk+, ωk-) for PRA-OXA (monomer), using Hirshfeld atomic charges

Sites	f_k^+	s_k^+	ωk+	**Sites**	f_k^-	s_k^-	ωk-
1 C	0.0715	0.0137	0.1494	1 C	0.0066	0.0013	0.0137
2 C	0.0472	0.009	0.0987	2 C	0.0086	0.0016	0.018
3 C	0.0541	0.0103	0.11307	3 C	0.0146	0.0028	0.0305
4 C	0.0723	0.0138	0.1511	4 C	0.0158	0.003	0.0331
5 C	0.0582	0.0111	0.12176	5 C	0.0216	0.0041	0.0451
6 C	0.0489	0.0093	0.10214	6 C	0.0365	0.007	0.0763
7 O	0.0931	0.0178	0.19457	7 O	0.0151	0.0029	0.0317
8 N	0.0459	0.0088	0.09603	8 N	0.0073	0.0014	0.0152
9 C	0.0294	0.0056	0.06141	9 C	0.0174	0.0033	0.0364
10 O	0.043	0.0082	0.08994	10 O	0.0112	0.0021	0.0233
11 C	0.0148	0.0028	0.03094	11 C	0.0512	0.0098	0.1071
12 H	0.023	0.0044	0.04811	12 H	0.0039	0.0007	0.0081
13 H	0.0313	0.006	0.06546	13 H	0.011	0.0021	0.023
14 H	0.0337	0.0064	0.07044	14 H	0.0308	0.0059	0.0644
15 H	0.0309	0.0059	0.06468	15 H	0.1256	0.024	0.2626
16 H	0.0359	0.0069	0.07499	16 H	0.0104	0.002	0.0217
17 H	0.0252	0.0048	0.05264	17 H	0.1272	0.0243	0.2658
18 H	0.0178	0.0034	0.03727	18 H	0.028	0.0053	0.0585
19 H	0.0137	0.0026	0.02865	19 H	0.124	0.0237	0.2592
20 H	0.0172	0.0033	0.03597	20 H	0.032	0.0061	0.0669
21 C	0.0178	0.0034	0.03715	21 C	0.0522	0.01	0.1092
22 O	0.0213	0.0041	0.0446	22 O	0.0326	0.0062	0.0682
23 O	0.0514	0.0098	0.10748	23 O	0.0579	0.0111	0.1211

24 C	0.019	0.0036	0.03976	24 C	0.0418	0.008	0.0874
25 O	0.0175	0.0034	0.03664	25 O	0.0215	0.0041	0.045
26 O	0.045	0.0086	0.09414	26 O	0.0522	0.01	0.1091
27 H	0.0166	0.0032	0.03462	27 H	0.0257	0.0049	0.0537
28 H	0.0043	0.0008	0.00903	28 H	0.0088	0.0017	0.0183